Proceedings of the 15th International Conference on Manufacturing Systems – ICMaS
Published by Editura Academiei Române, ISSN 1842-3183
"Politehnica" University of Bucharest, Machine and Manufacturing Systems Department
Bucharest, Romania, 26–27 October, 2006

METHOD OF SPRINGBACK COMPENSATION BASED ON THE OPTIMIZATION OF DEEP-DRAWING PROCESS

Crina AXINTE

Abstract: *The aim of this paper is to present a method which allows optimizing the tool geometry and the process parameters such that the resulted parts satisfy the accuracy demands. The analysis is performed in the case of cylindrical drawn parts and it is based on the Taguchi's method coupled to the finite element method.*

Key words: *optimization method, springback compensation, cylindrical drawn parts.*

1. INTRODUCTION

The final shape and dimensions of the formed parts are strongly affected by the springback phenomenon. In its turn, springback is a function of three main categories of factors, such as material properties, process parameters and tools geometry. Hence, by controlling all these factors, one should control the springback amount in order to obtain the desired accuracy of the formed parts. For this purpose, good results could be obtained from the application of some methods and techniques of optimization.

In this paper an optimization procedure based on the LMecA method is presented, in the case of cylindrical deep-drawing process. As result of the optimization procedure, virtual corrected tools are created, whose utilization, coupled with optimized process parameters, leads to a much lower springback, being thus fulfilled the conditions needed for proper manufacturing of the drawparts.

2. APPLICATION OF THE LMECA METHOD

The LMecA method was elaborated by a research team from University of Savoie, France, in order to compensate the springback of a V-bending part. The method is based on the Taguchi's method and assumes the following six stages:

1. Definition of the parameters that characterize the geometric deviations of the part.
2. Selection of the process parameter which can influence the geometry of the part, and their range of variation to test.
3. Choice of a linear or quadratic polynomial model and construction of an experiment design.
4. Performing the simulations defined by the experiment design and measurement of the geometrical defects on the obtained virtual parts.
5. Calculation of coefficients of the polynomial models and verification of the models.
6. Optimization of the process parameters in order to obtain the desired geometric parameters of the drawn parts.

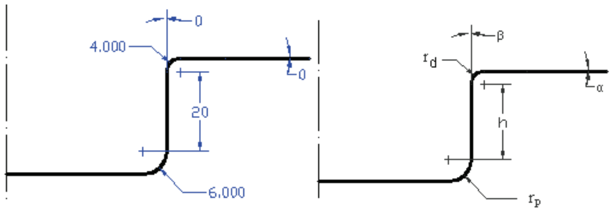

a b

Fig. 1. Geometric parameters of the cylindrical part: a – theoretical profile; b – analyzed geometric parameters.

2.1. Choice of the geometric parameters of part

The nominal geometry of the part and the geometric parameters whose variation will be investigated in order to quantify the effects of springback are presented in Fig. 1, where: r_d is the radius of connection between the part flange and part sidewall, r_p is the radius of connection between the part bottom and part sidewall, α is the angle of the flange, β is the inclination angle of part sidewall and h is the height of the part sidewall.

2.2. Choice of the process parameters

The initial configuration of tool is presented in Fig. 2.a. The used blankholder force was equal to 45 kN and the punch-die clearance was set to 1mm. The part resulted by using this configuration is presented in Fig. 2.b. Because the obtained values of geometrical parameters of the drawn part are different from the nominal ones, it follows to identify the process parameters that must be optimized in order to diminish the effect of springback.

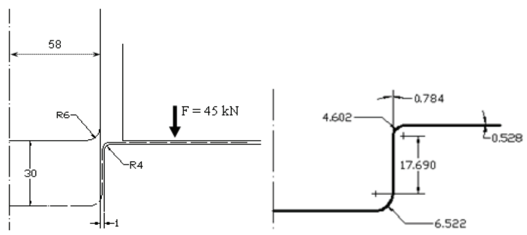

a. b.

Fig. 2. Geometry of tool and part: a – initial tool configuration; b – resulted part.

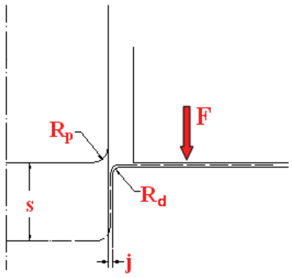

Fig. 3. Process parameters: R_p – punch radius; R_d – die radius; s – punch stroke; j – punch-die clearance; F – blankholder force.

Table 1

Tested process parameters and their fields of variation

Parameter	Initial value	Minimum value (–1)	Maximum value (+1)
Punch radius (R_p)	6 mm	5 mm	7 mm
Die radius (R_d)	4 mm	3 mm	5 mm
Blankholder force (F)	45 kN	40 kN	90 kN
Punch-die clearance (j)	1 mm	1 mm	1.5 mm
Punch stroke (s)	30 mm	30 mm	32 mm

These parameters and their fields of variation, chosen according to the initial simulation results and based on their probable influence on the part geometry, are presented in Fig. 3 and Table 1, respectively.

2.3. Choice of the model and construction of the experiments design

Two type of mathematical model are possible to link part parameters and process parameters:

- a polynomial model of the first degree, which supposes that the output Y varies linearly with each factor:

$$Y = a_0 + a_1x_1 + a_2x_2 + \ldots + a_nx_n + a_{12}x_1x_2 + \ldots + \\ + a_{n-1,n}x_{n-1}x_n \quad (1)$$

- a polynomial model of the second degree, which supposes that the output Y varies quadratically with each factor:

$$Y = a_0 + a_1x_1 + a_2x_2 + \ldots + a_nx_n + \ldots + a_{11}x_1^2 + \ldots + \\ + a_{nn}x_n^2 + a_{12}x_1x_2 + \ldots + a_{n-1,n}x_{n-1}x_n. \quad (2)$$

In each of the two models, Y represents the followed values (r_d, r_p, α, β, h), $x_1 \ldots x_n$ represent the values of the input parameters that must be optimized (R_p, R_d, F, j, s) and x_ix_j represent the interactions between the considered factors.

2.3.1. Linear optimization

Linear optimization assumes to identify a linear dependence between the part and process parameters. In order to determine the coefficients a_0, a_1, $a_2 \ldots a_n$ corresponding to each function, for the five analyzed factors, sixteen numerical experiments were needed to carry out as it is shown in Table 2. The result of each simulation was a file of nodes, representing the nodes of the virtual part mesh, after the tools removing. These files were post treated in order to measure the geometric part parameters. The results are given in Table 3.

Table 2

Factorial design for the linear dependence

Nº	R'_p	R'_d	F'	j'	s'
1	–1	–1	–1	–1	–1
2	–1	–1	–1	+1	+1
3	–1	–1	+1	–1	+1
4	–1	–1	+1	+1	–1
5	–1	+1	–1	–1	+1
6	–1	+1	–1	+1	–1
7	–1	+1	+1	–1	–1
8	–1	+1	+1	+1	+1
9	+1	–1	–1	–1	+1
10	+1	–1	–1	+1	–1
11	+1	–1	+1	–1	–1
12	+1	–1	+1	+1	+1
13	+1	+1	–1	–1	–1
14	+1	+1	–1	+1	+1
15	+1	+1	+1	–1	+1
16	+1	+1	+1	+1	–1

Table 3

Resulted parameters of part

Nº	r_p	r_d	α	β	h
1	5.613	3.673	0.928	0.252	20.654
2	5.648	3.388	0.742	1.192	22.922
3	5.608	3.388	0.742	1.192	22.964
4	5.589	3.525	0.938	1.565	20.619
5	5.548	5.399	0.618	0.261	20.926
6	5.738	5.436	0.523	1.342	18.750
7	5.589	5.456	0.185	0.368	18.923
8	5.662	5.396	0.627	1.304	20.849
9	7.503	3.494	1.031	0.158	20.912
10	7.499	3.385	0.909	1.443	18.944
11	7.558	3.350	0.909	1.443	18.984
12	7.594	3.396	0.728	1.424	20.947
13	7.443	5.437	0.476	0.348	16.978
14	7.525	5.437	0.306	1.382	18.910
15	7.485	5.494	0.313	0.348	18.971
16	7.560	5.524	0.444	1.784	16.833

From the results of the experiment design, the coefficients of polynomial model of each output were calculated. The following equations were got:

$$r_p = 6.472 + 0.948R'_p - 0.004R'_d + 0.008F' + 0.029j' - \\ -0.001s' - 0.014R'_pR'_m + 0.02R'_pF' - 0.01R'_pj' + \\ +0.007R'_ps' - 0.001R'_dF' + 0.023R'_dj' - 0.01R'_ds' - \\ -0.01F'j' + 0.008F's' + 0.006j's' \quad (3)$$

$$r_p = 4.448 - 0.009R'_p + 0.099R'_d - 0.008F' - 0.013j' - \\ -0.025s' + 0.035R'_pR'_d + 0.009R'_pF' + 0.009R'_pj' + \\ +0.04R'_ps' + 0.028R'_dF' + 0.014R'_dj' + 0.009R'_ds' + \\ +0.032F'j' + 0.002F's' - 0.01j's' \quad (4)$$

$$\alpha = 0.651 - 0.012R'_p - 0.215R'_d - 0.04F' + 0.001j' - \\ -0.013s' - 0.04R'_pR'_d - 0.001R'_pF' - 0.04R'_pj' - \\ +0.03R'_ps' - 0.001R'_dF' + 0.038R'_dj' + 0.042R'_ds' + \\ +0.073F'j' + 0.005F's' - 0.04j's' \quad (5)$$

$$\beta = 0.687 - 0.053R'_p - 0.096R'_d + 0.191F' + 0.442j' - \\ -0.08s' + 0.02R'_pR'_d + 0.018R'_pF' + 0.025R'_pj' - \\ -0.13R'_ps' - 0.13R'_dF' + 0.119R'_dj' + 0.012R'_ds' - \\ -0.1F'j' - 0.03F's' - 0.02j's' \quad (6)$$

Table 4

Comparison of the results

	R'_p	R'_d	F'	j'	s'	Values obtained from relations (1÷5)	Values obtained from simulation	Errors
r_p	0	0	0	0	0	6.472	6.416	0.056
r_d	0	0	0	0	0	4.448	4.462	–0.014
α	0	0	0	0	0	0.651	0.535	0.116
β	0	0	0	0	0	0.687	0.539	0.148
h	0	0	0	0	0	19.880	19.625	0.255

$$\begin{aligned} h = {} & 19.880 - 0.946R'_p - 0.988R'_d + 0.006F' - 0.034j' + \\ & +1.045s' - 0.024R'_pR'_d - 0.01R'_pF' + 0.007R'_pj' - \\ & -0.04R'_ps' - 0.001R'_dF' - 0.02R'_dj' - 0.02R'_ds' - \\ & -0.04F'j' + 0.002F's' + 0.015j's' \end{aligned} \tag{7}$$

In order to test the assumption of the output's linearity, a numerical simulation was carried out at the centre of the variation field ($R_p = 6$ mm, $R_d = 4$ mm, $F = 65$ kN, $j = 1.25$ mm and $s = 31$ mm). The results of the simulation were compared with those obtained using the relations (1÷5) and are presented in Table 4.

By analyzing the above presented results some differences could be observed between the two modalities of determination. Hence, the precision of the model could be improved by choosing a quadratic model.

2.3.2. Quadratic optimization

In order to determine the coefficients of the quadratic model a number of 10 additional simulations were needed (Table 5). The results of simulations are given in Table 6.

Table 5

Factorial design for the linear dependence

N°	R'_p	R'_d	F'	j'	s'
1	–1.719	0	0	0	0
2	+1.719	0	0	0	0
3	0	–1.719	0	0	0
4	0	+1.719	0	0	0
5	0	0	–1.719	0	0
6	0	0	+1.719	0	0
7	0	0	0	–1.719	0
8	0	0	0	+1.719	0
9	0	0	0	0	–1.719
10	0	0	0	0	+1.719

Table 6

Resulted parameters of part

N°	r_p	r_d	α	β	h
1	4.793	4.307	0.801	0.831	21.799
2	8.402	4.457	0.709	1.378	18.017
3	6.535	3.310	0.647	0.949	21.082
4	6.627	6.176	0.088	1.116	18.151
5	6.545	4.355	0.580	0.107	20.049
6	6.661	4.446	0.580	0.818	19.808
7	6.528	4.340	0.406	1.197	18.336
8	6.696	4.439	0.528	1.971	19.808
9	6.626	4.450	0.612	0.859	21.606
10	6.701	4.439	0.528	1.844	19.803

The first sixteen experiments coupled with these ten new experiments allowed to calculate the coefficients of the quadratic model:

$$\begin{aligned} r_p = {} & 6.378 + 0.975R'_p + 0.004R'_d + 0.015F' + 0.034j' + \\ & +0.005s' - 0.014R'_pR'_d + 0.020R'_pF' - 0.006R'_pj' + \\ & +0.007R'_ps' - 0.001R'_dF' + 0.023R'_dj' - 0.01R'_ds' - \\ & -0.01F'j' + 0.008F's' + 0.006j's' - 0.02R'^2_p - \\ & -0.02R'^2_d - 0.013F'^2 - 0.01j'^2 + 0.007s'^2 \end{aligned} \tag{8}$$

$$\begin{aligned} r_d = {} & 4.417 + 0.005R'_p + 0.954R'_d + 0.001F' - 0.001j' - \\ & -0.019s' + 0.034R'_pR'_d + 0.008R'_pF' + 0.008R'_pj' + \\ & +0.04R'_ps' + 0.028R'_dF' + 0.014R'_dj' + 0.009R'_ds' + \\ & +0.032F'j' + 0.002F's' - 0.01j's' - 0.03R'^2_p + \\ & +0.091R'^2_d - 0.025F'^2 - 0.029j'^2 - 0.01s'^2 \end{aligned} \tag{9}$$

$$\begin{aligned} \alpha = {} & 0.501 - 0.015R'_p - 0.202R'_d - 0.03F' + 0.010j' - \\ & -0.016s' - 0.04R'_pR'_d - 0.001R'_pF' - 0.044R'_pj' - \\ & -0.03R'_ps' - 0.001R'_dF' + 0.038R'_dj' + 0.042R'_ds' + \\ & +0.073F'j' + 0.005F's' - 0.04j's' + 0.097R'^2_p - \\ & -0.03R'^2_d + 0.037F'^2 - 0.001j'^2 + 0.034s'^2 \end{aligned} \tag{10}$$

$$\begin{aligned} \beta = {} & 0.593 + 0.081R'_p - 0.056R'_d + 0.19F' + 0.383j' + \\ & +0.018s' + 0.019R'_pR'_d + 0.017R'_pF' + 0.025R'_pj' - \\ & -0.013R'_ps' - 0.013R'_dF' + 0.119R'_dj' + 0.012R'_ds' - \\ & -0.1F'j' - 0.03F's' - 0.02j's' + 0.02R'^2_p - \\ & -0.001R'^2_d - 0.198F'^2 + 0.181j'^2 + 0.103s'^2 \end{aligned} \tag{11}$$

$$\begin{aligned} h = {} & 19.899 - 0.987R'_p - 0.951R'_d - 0.014F' + 0.091j' + \\ & +0.621s' - 0.024R'_pR'_d - 0.007R'_pF' + 0.007R'_pj' - \\ & -0.04R'_ps' - 0.001R'_dF' - 0.02R'_dj' - 0.02R'_ds' - \\ & -0.04F'j' + 0.002F's' + 0.015j's' + 0.016R'^2_p - \\ & -0.08R'^2_d + 0.023F'^2 - 0.267j'^2 + 0.285s'^2 \end{aligned} \tag{12}$$

In order to test the above presented relations a simulation was carried out at the centre of the variation field ($R_p = 6$ mm, $R_d = 4$ mm, $F = 65$ kN, $j = 1.25$ mm and $s = 31$ mm). The results of the simulation were compared with those obtained using the relations (6÷10) and are presented in Table 7.

Table 7

Comparison of the results

	R'_p	R'_d	F'	j'	s'	Values obtained from relations (6÷10)	Values obtained from simulation	Errors
r_p	0	0	0	0	0	6.378	6.416	–0.038
r_d	0	0	0	0	0	4.417	4.462	–0.045
α	0	0	0	0	0	0.501	0.535	–0.034
β	0	0	0	0	0	0.593	0.539	0.054
h	0	0	0	0	0	19.899	19.625	0.274

From the comparative analysis, a diminution of the differences between the values obtained from the two modalities of determination could be observed; in consequence, the quadratic model will be used to determine the optimum values of process parameters which allow to

Table 8

Optimum values of the tool geometry/ process parameters

	R_p [mm]	R_d [mm]	F [kN]	j [mm]	s [mm]	r_p [mm]	r_d [mm]	α [°]	β [°]	h [mm]
Values resulted from optimization	5.56	3.62	48	1	31.90	6.122	3.988	0.328	0.411	19.936

Table 9

Comparative analysis of the results

	R_p [mm]	R_d [mm]	F [kN]	j [mm]	s [mm]	r_p [mm]	r_d [mm]	α [°]	β [°]	h [mm]
Values resulted by using initial tools design	6	4	45	1	30	6.522	4.602	0.528	0.784	17.69
Values resulted from quadratic model	5.56	3.62	48	1	31.90	6.122	3.988	0.328	0.411	19.936
Values resulted from simulation						6.105	4.062	0.286	0.405	20.122
Nominal values						6.000	4.000	0.000	0.000	20.000

obtain the best values for the geometrical parameters of part (as close as possible to the target values).

2.4. Optimization of the tool geometry and process parameters

The principle consists in minimizing a function equal to the squared sum of deviation between the theoretical and the desired output:

$$\Phi = \left(r_p - 6\right)^2 + \left(r_d - 4\right)^2 + \left(\alpha - 0\right)^2 + \left(\beta - 0\right)^2 + \left(h - 20\right)^2 \qquad (13)$$

This function has several local minima. The Excel solver was used to seek them. In the field of study, defined by the value (–1) and the value (+1) of the process parameters, none of these minima is equal to zero. In other words, it is not possible to obtain the five wished values for the part parameters simultaneously. The lowest minimum on this field is given in Table 8.

In order to validate the optimization algorithm a new simulation was performed, using as input data the above optimized process parameters and tool geometry. The results of quadratic optimization, of finite element simulation and the nominal values of the geometrical parameters of part are compared in Table 9.

A good concordance between the estimated values by minimizing the function Φ and that obtained from simulation could be observed. Also, the accuracy of part obtained by using the optimized process parameters/tool geometry is much improved compared to that obtained by using the initial process parameters/tool configuration.

The corrected geometry of tool and the drawn part resulted by using this geometry are presented in Fig. 4 and Fig. 5, respectively.

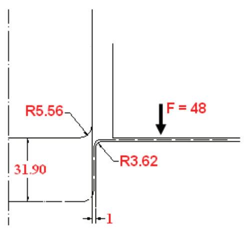

Fig. 4. Optimized tool geometry/process parameters.

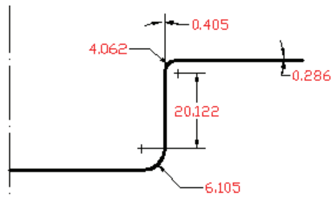

Fig. 5. Resulted geometry of the part.

3. CONCLUSIONS

In order to diminish the effect of springback on the part geometrical accuracy, an optimization procedure based on the LMecA method coupled with the finite element method was presented. The proposed method allows optimizing the tools geometry and process parameters in order to compensate the elastic deflections of the part.

Good results were obtained by using the quadratic model. As result of the performed optimization, the deviations of geometrical parameters of the part reported to the nominal profile decreased as follows: with 78.5% for the radius of connection between the part bottom and part sidewall r_p, with 88.3% for the radius of connection between the part flange and part sidewall r_d, with 94.8% for the height of the part sidewall h, with 54.2% for the flange angle α and with 51.7% for the sidewall inclination angle β.

As a consequence, the presented method could be successfully used to control the springback phenomenon in the case of cylindrical drawn parts.

REFERENCES

[1] Arrieux, R. *et al.* (2005). *A method of springback compensation based on finite element method and design of experiment*, INETFORSMEP, Conference Proceedings, Poznan-Wasowo, Poland, pp. 69–83.

[2] Axinte, C. (2006). *Theoretical and experimental researches concerning the springback phenomenon in the case of cylindrical deep-drawn parts*, Ph.D. Thesis.

Author:

Crina AXINTE, Assistant professor, University of Bacău, Faculty of Engineering, E-mail: crina.axinte@gmail.com